Chemistry–A European Journal
Research Article
doi.org/10.1002/chem.202103830
Chemistry Europe
European Chemical Societies Publishing
www.chemeurj.org

Comparative Study of Nitro- and Azide-Functionalized Zn^{II}-Based Coordination Polymers (CPs) as Fluorescent Turn-On Probes for Rapid and Selective Detection of H_2S in Living Cells

Subhajit Saha,[a] Pritam Kumar Roy,[b] Kartik Maity,[a] Mahitosh Mandal,[b] and Kumar Biradha*[a]

Abstract: Selective detection of H_2S in the cellular systems using fluorescent CPs/MOFs is of great scientific interest due to their outstanding aqueous stability, biocompatibility and real-time detection ability. Fabrication of such materials using complete biologically essential elements and applying them as an efficient biosensor is still quite challenging. In this context, two newly synthesized CPs containing biologically essential metal ion (Zn) and nitro/azido functional groups into the framework to sense extracellular and intracellular H_2S by reducing into respective amines are presented. The CP-**1** containing the azide group acted as an efficient fluorescent turn-on probe with the lowest detection limit (7.2 μM) and shortest response time (30 s) among the Zn-based probes reported till date. Moreover, CP-**1** exhibited green luminescence in live cells after imaging a very low concentration of H_2S, whereas the nitro analogue CP-**2** could not detect the target analyte due to its framework disruption.

Introduction

Hydrogen sulfide (H_2S), highly toxic gas with a distinct rotten egg smell, has attracted great attention for its signalling role in biological systems and pathological processes.[1] The major source of this gas is chemical and pharmaceutical industries, including petroleum refining and natural gas production. Besides that, our body also acts as a minor source through decomposing the sulfur-containing organic compounds.[2] Thus, in biological medium, concentration of H_2S gas at nanomolar to micromolar level is satisfactory, but higher concentration results in unconsciousness, critical poisoning, swift apnea, inactivation of the olfactory system (30–40 ppm H_2S), and even death ($\geq$250 ppm H_2S).[3] Several diseases like Alzheimer's, Parkinson's, diabetics, Down's syndrome, cancer are also related to the cause of the abnormal level of H_2S.[4] Therefore, the fast identification and quantification of H_2S are necessary with high sensitivity and simplicity. Keeping this in mind, the fluorescence-based sensing method has gained significant scientific interest over the other traditional detection methods such as colorimetry, electrochemical analysis, gas chromatography and sulfide precipitation.[5] An ideal fluorescent probe must work in 'turn-on' manner with high signal-to-noise ratio and high selectivity. For selective detection of hydrogen sulfide, few mechanisms have been reported so far, such as reduction of azide/nitro groups into amines, cleavage of double bonds *via* nucleophilic addition, removal of Cu^{2+} ions as CuS and coordinative based approach. Highly conjugated organic molecules containing azide/nitro/C=C functional groups have been shown as H_2S sensors based on their reactivity with sulphide ions.[6] Further, many transition metal complexes were also shown as an advanced H_2S sensors by reversible binding of sulphide ions with the metal site.[7] In recent years, metal–organic frameworks (MOFs) or coordination polymers (CPs) have been widely used for quantitative detection of various analytes due to their chemical stability, adjustable porosity and possibility for post-synthetic modification (PSM).[8] Tailoring the electronic properties of the coordinating ligands and applying PSM, numerous MOF-based fluorescent sensors for selective H_2S detection have been documented to date (Table S4).[9] Several of these studies, about 80%, deal with highly toxic (Pb, Cd and lanthanides) and non-essential metal ions (Al and Zr), limiting their applicability for *in-vivo* bioimaging (Figure 1).[10] The rest of the 20% MOFs are with essential metal ions, like Zn, Cu and Fe, but their lower detection limits are not up to those of other elements. Therefore, it is important to design and synthesize MOFs, containing essential metal ions to serve as fluorescent 'turn-on' probes with lower detection limits.

Recently, we have reported a series of CPs containing bis-pyridyl amide functionalities and their potential application in sensing, selective guest inclusion, proton conductivity and

[a] S. Saha, K. Maity, Prof. K. Biradha
Department of Chemistry
Indian Institution of Technology Kharagpur
Kharagpur 721302 (India)
E-mail: kbiradha@chem.iitkgp.ernet.in
[b] P. K. Roy, Prof. M. Mandal
School of Medical Science and Technology
Indian Institution of Technology Kharagpur
Kharagpur 721302 (India)

Supporting information for this article is available on the WWW under https://doi.org/10.1002/chem.202103830

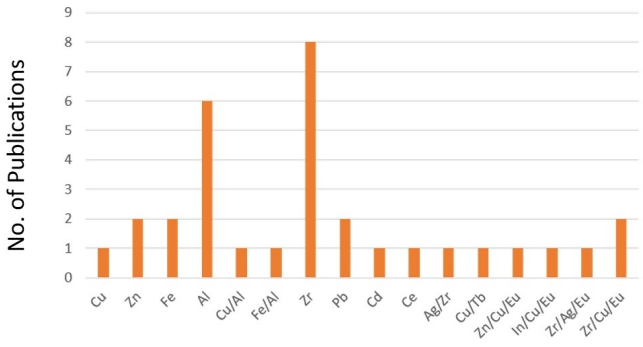

Figure 1. Statistical representation of MOFs/CPs containing various metal ions studied for H_2S sensing.

dye removal.[11] The advantage of choosing bis-pyridyl ligands containing the amide and aromatic and/or aliphatic spacers is to fulfill the coordination requirement of central metal ions and strong hydrogen bonding interaction from the amide groups. On the other hand, polycarboxylic acids with multiple coordination modes as O-donor ligands are outstanding co-ligands in the construction of CPs.[12] Herein, we wish to present two new Zn(II) CPs containing flexible bis-pyridyl-bis-amide ligand, N,N′-bis(4-methylenepyridine-4-yl)-1,4-benzenedicarboxamide (**4-bmpbd**), and nitro/azido substituted isophthalates as co-ligands (Scheme 1). The Zn(II) CPs, CP-**1** and CP-**2**, are aimed at effective detection of H_2S by reducing the nitro and azido groups into amines. Although CP-**1** and CP-**2** are isostructural, they were found to exhibit distinguishable photoluminescence properties in dispersed phase. CP-**1** shows rapid and selective turn-on response towards H_2S, while CP-**2** fails in terms of sensitivity and selectivity in the presence of other potentially competing biomolecules. The capability of CP-**1** has also been tested through live-cell imaging studies to detect intracellular H_2S. As compared to the previously reported Zn-MOF based fluorescent probes, the detection limit of CP-**1** is the lowest fluorescent turn-on probe reported till date in aqueous medium.

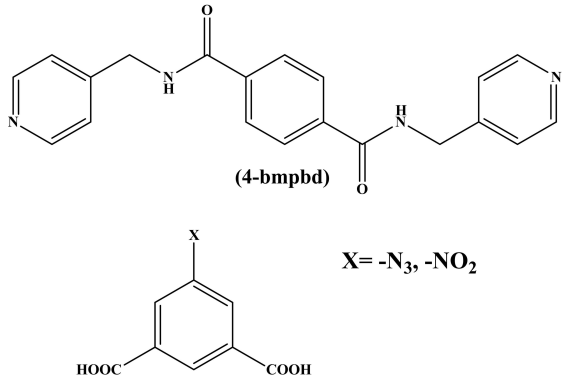

Scheme 1. Chemical structures of ligand and co-ligands.

Results and Discussion

The CPs are synthesized by solvothermal reactions by taking the equimolar amounts of 4-bmpbd, $Zn(NO_3)_2$ and corresponding isophthalic acids, such as 5-azidoisophthalic acid (H_2AIP) and 5-nitroisophthalic acid (H_2NIP). The single crystal X-ray diffraction analyses reveal that the CP-**1** and CP-**2** have the formulae of $\{[Zn(4\text{-bmpbd})(AIP)].2H_2O\}_n$ and $\{[Zn(4\text{-bmpbd})(NIP)].2H_2O\}_n$, respectively. The crystal structure analyses suggest that these two CPs are isostructural and contain 1D-coordination network. CP-**1** crystallized in triclinic *P-1* space group and the asymmetric unit is composed of one each of Zn(II) ion, 4-bmpbd and IPA unit and two uncoordinated water molecules. The Zn(II) centre was found to exhibit distorted tetrahedral geometry, where two carboxylates and two 4-bmpbd units were present at the four coordination sites (Figure 2a). The bond lengths and bond angles are given in Table S2. This type of coordination and angular nature of the ligand resulted in the formation of M_2L_2 macrocycle with the dimension of 16.4×11.1 Å^2 (Figure 2b). These macrocycles were further interconnected by IPA units to form a tubular structure, where the macrocycles were separated by a distance of 10.17 Å. Within the tube, two water molecules are hydrogen-bonded (O···O: 2.923(10) Å) to form a dimer and connects the amide groups of macrocycles *via* N–H···O (N···O: 3.109(9) Å, 152°) and O–H···O (O···O: 3.042(9) Å) hydrogen bonds (Figure 2c). These 1D-tubular networks were further polycatenated to give a remarkable two-dimensional layer (Figure 2d). The tubes were interweaved in a parallel fashion *via* N–H···O hydrogen bonding (N···O: 2.929(7) Å, 155°) between the amide N–H and the carboxylate of isophthalate. Through these interactions, each tube was polycatenated by two neighbouring tubes to fill the void space (Figure S1a). In addition, these polycatenated sheets are further stacked on each other *via* weak face-to-face aromatic interactions (centroid-centroid: 3.9 Å) between the central phenylene ring of ligands (Figure S1b). The crystal structure of CP-**2** is also found to have similar types of interactions given its isostructurality with that of CP-**1** (Figure S2). Detailed geometrical parameters of hydrogen bonds have been given in Table S3.

As was mentioned previously, the azido and nitro groups were placed in CPs to use as fluorescent probes for selective H_2S sensing. The reduction of $-N_3$ or $-NO_2$ groups of CPs to electron-donating amino group is anticipated to turn on fluorescence intensity. Therefore, the two CPs are explored for H_2S sensing by conducting fluorescence turn-on experiments in the dispersed phase. Firstly, the stability of CPs was examined by immersing them in water for four days and recording powder X-ray diffraction (PXRD). No significant change in the PXRD pattern was found, indicating their structural integrity (Figure S3). For sensing experiments, a stock solution was prepared by dispersing 0.5 mg (77 μmol) finely ground powder of CPs in 10 ml of water. These suspensions were excited at a wavelength (λ_{ex}) of 300 nm (Figure S4b) and all the fluorescence spectra were recorded in the range of 350–580 nm. The azido-functionalized CP-**1** exhibited weak fluorescence at 400 nm with a shoulder band at 500 nm. The band at 400 nm can be

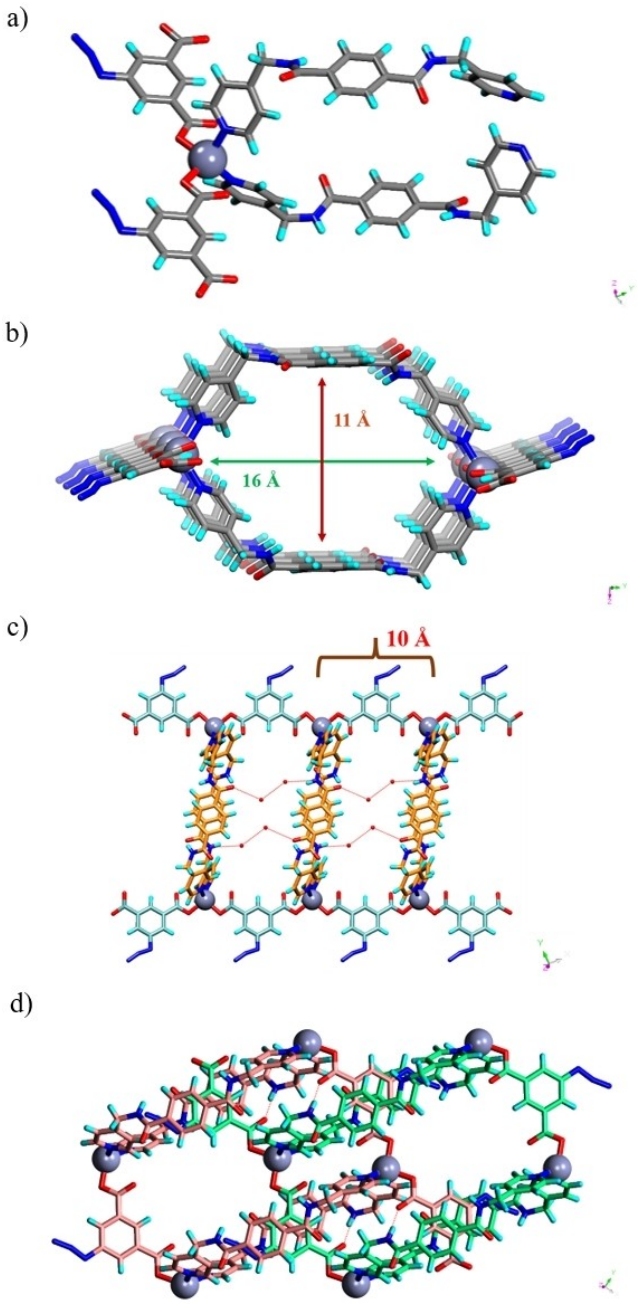

Figure 2. Illustrations for the crystal structure of CP-**1**: (a) coordination environment of Zn(II); (b) 1D-tubular coordination network by formation of M_2L_2 macrocycles; (c) side view of 1D-tubular network by linking of macrocycles by IPA units and linear water chains; (d) hydrogen bonding between entangled tubular networks (side view).

attributed to ligand-based emission originated from π-π* transition (Figure S6a), whereas the red-shifted band at 500 nm is due to the complexation of ligand with the metal ion.[11a] In order to investigate the detection performance, aqueous solution of Na_2S was added as a source of H_2S and monitored the fluorescence intensity. Interestingly, such an addition was found to result in an immediate enhancement of fluorescence by 3-fold (Figure 3a, S5), which indicates the better utility of CP-**1** for the real-time intracellular H_2S imaging compared to other reported probes, using reduction mechanism, till date.[13] The quantitative fluorescence response was further investigated by varying concentrations of Na_2S (up to 10 equivalents/azide group). The saturation in emission intensity was observed after the addition of 6 equivalents of Na_2S. Along with saturation, a slight diminution in intensity at higher wavelength was also observed (Figure 3b). Very high sulfide concentration was eventually found to disrupt the polymeric network by coordinating with the Zn-metal sites, which was confirmed by PXRD analysis (Figure S10b).[14] As shown in Figure 3c, an excellent linear relationship ($R^2 = 0.9899$) of the fluorescence intensity (I_{400}) with sulfide concentration can be established in the concentration range of 0—1 equivalent. From the linear curve, the slope was calculated to be 41.3 with an intercept of 5873. Using this slope value(S) and the standard deviation of blank solution(δ), the limit of detection (LOD = 3δ/S, where 3 is the factor of 99% confidence level) value of CP-**1** toward sulfide was calculated to be 7.2 μM. This detection limit is quite impressive as MOF-based fluorescence turn-on sensor particularly with the essential element Zn(II).[15]

For a chemosensor, selectivity is another important index towards every target analyte. Thus, it is necessary to check the selectivity of CP-**1** for H_2S over potentially interfering biomolecules (such as serine, glutathione, cysteine and alanine) and some common reducing anions (such as $NaNO_2$, $NaNO_3$, NaCl, NaBr and NaI). Five equivalents of each analyte per azide functionality were tested individually and found that only cysteine is a close competitor to the target analyte H_2S among all (Figure 3d). For efficient selectivity in a complicated biological medium, H_2S needs to be detected even in the presence of other potentially intrusive analytes. Therefore, after individual inspection of each analyte, five equivalents of Na_2S were added to these solutions and found significant fluorescence turn-on response even in the presence of interfering congeners. These results demonstrate that CP-**1** can recognize H_2S very effectively in complex biological systems avoiding off-target reactivity and false response. Thus, in continuation of extracellular study in 100% aqueous medium, H_2S detection in the biological medium was further investigated in LN-18 glioblastoma cells. Treating the cells with different concentrations of CP-**1** (0-100 μM) and observing in the bright field revealed no alteration of cellular morphology as we deliberately chose essential element Zn for our cellular studies (Figure 4a,c). When the cells were incubated with only 10 μM of probe (CP-**1**) for 48 h no fluorescence was observed, but only addition of 5 μM of Na_2S solution as an intracellular H_2S generator the fluorescence was observed in the green channel maintaining the intact morphology (Figure 4b,d). The turn-on emission band at 500 nm might be responsible for the respective fluorescence in cellular system and it can be inferred that newly synthesized CP-**1** is surely accomplished for recognizing intracellular H_2S.

To ensure the framework stability and conversion of azide group into amines after sulfide detection, some experiments were performed such as PXRD, FTIR and ^{1}H NMR spectroscopic analyses. The PXRD patterns of CP-**1** before and after the H_2S sensing experiments are very similar, which excludes the possibility of structural collapse after reducing the azide group

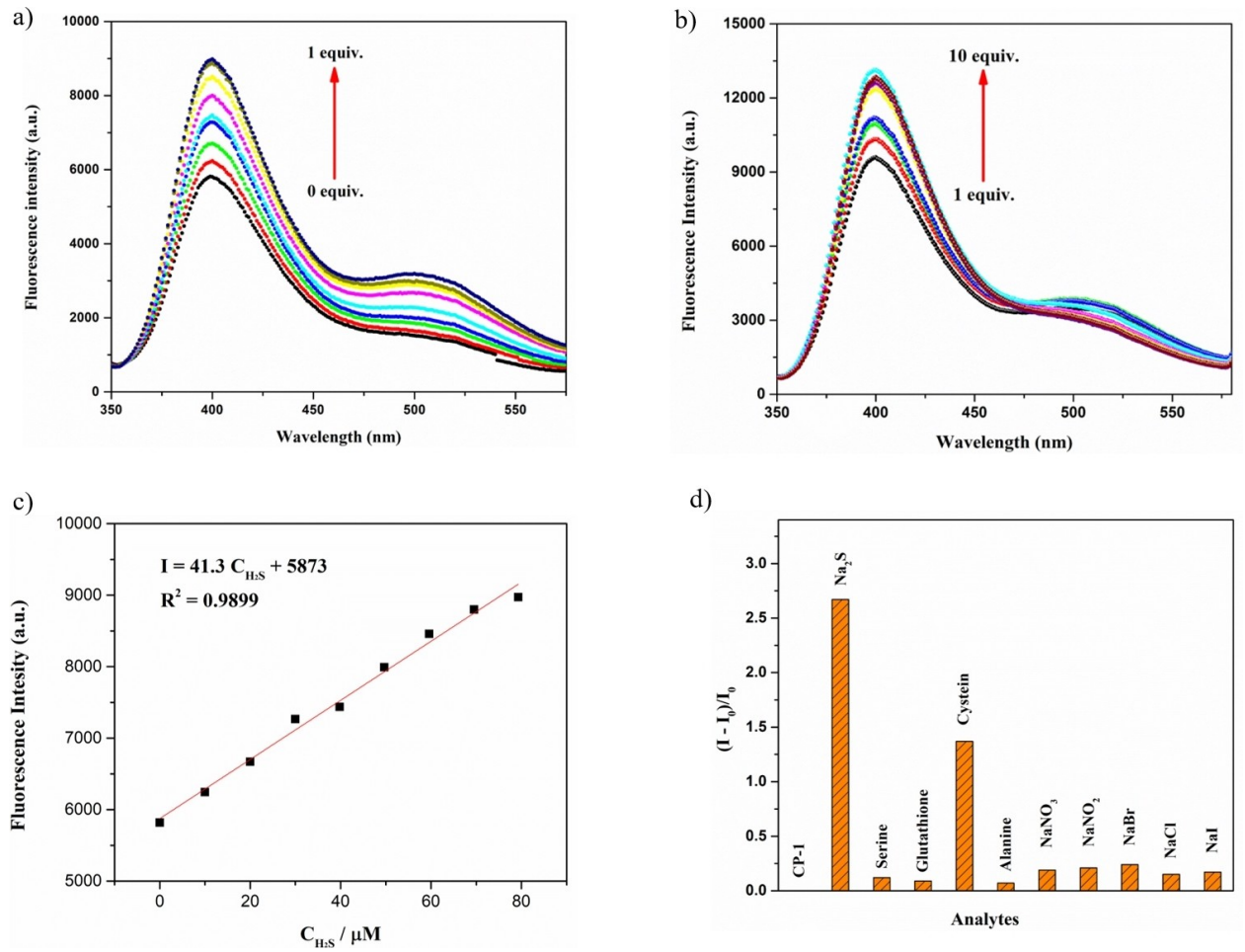

Figure 3. Concentration-dependent fluorescence turn-on response of CP-**1** upon addition of Na_2S up to 1 equivalent; (b) further addition up to 10 equiv. of Na_2S; (c) concentration dependence fitting curve (0 to 1 equiv); (d) comparative fluorescence response of CP-**1** towards different analytes (5 equiv).

(Figure S10a). The FTIR spectrum was recorded with similar sets of material and observed a clear change in spectra after the treatment. A sharp peak at 2101 cm^{-1} corresponding to the azide functionality disappeared in the Na_2S-treated probe and a broad peak appeared in the range of 2750–3650 cm^{-1} due to the formation of -NH_2 group (Figure S11). From the ^1H NMR analysis; the formation of amino isophthalic acid was also confirmed with the appearance of a corresponding broad peak for protonated amines (-NH_3^+) at 13.46 ppm (Figure S9). A slight shift in the position of aromatic proton peaks (7-9 ppm) was also observed for the sulfide treated CP-**1**, suggesting the chemical modification in the polymeric framework. Here we would like to note that these type of probes are not reusable, although the network is intact but the azide groups are converted to amines. Therefore, the efforts are made to convert the amine to azide by treating with $TMSN_3$ and tBuONO in THF. However, the CP-**1** was found to disintegrate under the above conditions. The nitro analogue, CP-**2**, was also expected to exhibit a similar ability for H_2S detection as it contains nitro groups as an electron-withdrawing group instead of azido. However, studies on CP-**2** indicate no significant turn-on emission with the addition of aqueous Na_2S solution. Even the addition of 100 equivalent of Na_2S didn't result in significant enhancement of the emission intensity and exhibited very high LOD value of 0.8 mM (Figure S7). The only emission band at 432 nm was too weak to detect H_2S with high selectivity and low quantity, which indicates that CP-**2** is not an efficient H_2S detector. To find out the probable reason for such different behaviour from CP-**1**, PXRD analysis was performed for CP-**2** after treating with two equivalents of Na_2S solution. The PXRD pattern indicates a complete disruption of network (Figure S12).

Conclusion

Two new Zn^{II} CPs have been synthesized with semi-rigid dipyridyl ligand (**4-bmpbd**) and two rigid dicarboxylates under solvothermal condition. Both CPs are isostructural with the formation of 1D-tubuler channel through distorted tetrahedral coordination network. Further polycatenation of these tubular channels gives a 2D-layered structure, driven by the plethora of N–H···O hydrogen bonding between the ligand and co-ligands. Using these less toxic and water-stable materials, detection of H_2S in the micromolar level can be achieved by 'turn-on'

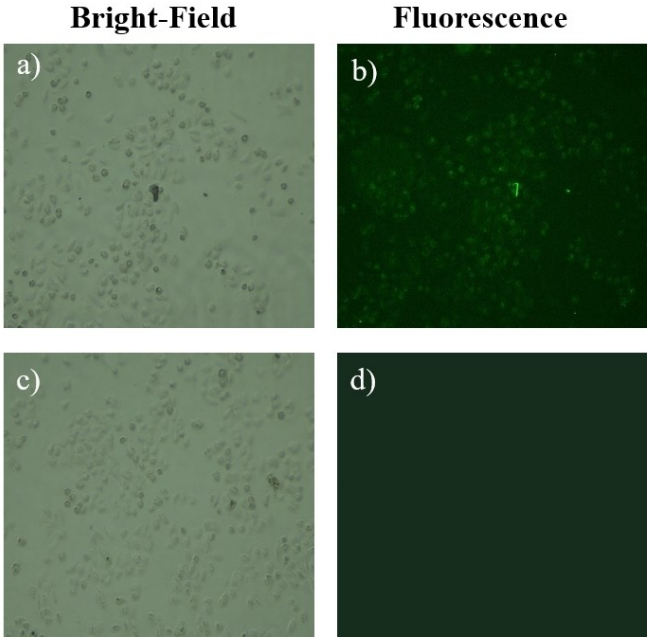

Figure 4. Intracellular behaviour of CP-**1** in LN-18 glioblastoma cells: bright field image of probe-loaded cells before (a) and after (c) treating with Na_2S solution; fluorescence image of respective cells before (b) and after (d) treating with Na_2S solution.

mechanism in extracellular, as well as intracellular systems. Among the existing Zn-based sensors, CP-**1** is found to be the most sensitive fluorescent 'turn-on' probe (LOD = 7.2 μM) towards H_2S to date. The use of essential metal ions with simple organic molecules is a better strategy for the development of bio-compatible H_2S sensors. Rapid enhancement of fluorescence intensity caused due to the reduction of azide group, whereas the nitro group of CP-**2** remains unreactive towards H_2S. To realize the full potential of CP-based heterogenous H_2S sensors, the designed CPs should have the recyclability, which have not been reported to date, our group is working in this direction.

Experimental Section

All the synthetic procedures, characterization spectra and experimental plots are provided in the Supporting Information. Deposition Numbers 2115567 (for CP-**1**), 2115568 (for CP-**2**) contain the supplementary crystallographic data for this paper. These data are provided free of charge by the joint Cambridge Crystallographic Data Centre and Fachinformationszentrum Karlsruhe Access Structures service.

Acknowledgements

We gratefully acknowledge DST-SERB (EMR/2017/001499), New Delhi, India for financial support, DST-FIST for the single crystal X-ray diffractometer. MM acknowledges Indian Council of India, New Delhi, UGC, Govt of India and SERB India for providing the JC Bose Fellowship. SS thanks CSIR for fellowship.

Conflict of Interest

The authors declare no conflict of interest.

Data Availability Statement

The data that support the findings of this study are available in the supplementary material of this article.

Keywords: cell imaging · coordination polymers · essential elements · fluorescence · H_2S sensors

[1] R. J. Reiffenstein, W. C. Hulbert, S. H. Roth, *Annu. Rev. Pharmacol. Toxicol.* **1992**, *32*, 109–134.
[2] T. L. Guidotti, *Int. J. Toxicol.* **2010**, *29*, 569–581.
[3] C. Meng, X. Cui, S. Qi, J. Zhang, J. Kang, H. Zhou, *Surgery* **2017**, *161*, 1287–1298.
[4] a) K. Eto, T. Asada, K. Arima, T. Makifuchi, H. Kimura, *Biochem. Biophys. Res. Commun.* **2002**, *293*, 1485–1488; b) P. Kamoun, M. C. Belardinelli, A. Chabli, K. Lallouchi, B. Chadefaux-Vekemans, *Am. J. Med. Genet. Sect. A* **2003**, *116*, 310–311; c) C. Szabo, *Antioxid. Redox Signaling* **2012**, *17*, 68–80.
[5] a) X. Zhang, Q. Zhang, D. Yue, J. Zhang, J. Wang, B. Li, Y. Yang, Y. Cui, G. Qian, *Small* **2018**, *14*, 1801563–1801569; b) M. K. Smith, K. A. Mirica, *J. Am. Chem. Soc.* **2017**, *139*, 16759–16767; c) J. Cui, Y.-L. Wong, M. Zeller, A. D. Hunter, Z. Xu, *Angew. Chem. Int. Ed.* **2014**, *53*, 14438–14442; *Angew. Chem.* **2014**, *126*, 14666–14670; d) M. G. Choi, S. Cha, H. Lee, H. L. Jeon, S. K. Chang, *Chem. Commun.* **2009**, *47*, 7390–7392; e) N. S. Lawrence, J. Davis, L. Jiang, T. G. J. Jones, S. N. Davies, R. G. Compton, *Electroanalysis* **2000**, *12*, 1453–1460.
[6] a) F. Yu, X. Han, L. Chen, *Chem. Commun.* **2014**, *50*, 12234–12249; b) N. Kumar, V. Bhalla, M. Kumar, *Coord. Chem. Rev.* **2013**, *257*, 2335–2347; c) V. S. Lin, C. J. Chang, *Curr. Opin. Chem. Biol.* **2012**, *16*, 595–601.
[7] a) M. Strianese, C. Pellecchia, *Coord. Chem. Rev.* **2016**, *318*, 16–28; b) E. Galardon, A. Tomas, M. Selkti, P. Roussel, I. Artaud, *Inorg. Chem.* **2009**, *48*, 5921–5927; c) E. Galardon, A. Tomas, P. Roussel, I. Artaud, *Dalton Trans.* **2009**, *42*, 9126–9130; d) M. Strianese, A. Varriale, M. Staiano, C. Pellecchia, S. D'Auria, *Nanoscale* **2011**, *3*, 298–302; e) M. D. Hartle, S. K. Sommer, S. R. Dietrich, M. D. Pluth, *Inorg. Chem.* **2014**, *53*, 7800–7802; f) M. Strianese, M. Lamberti, C. Pellecchia, *Dalton Trans.* **2018**, *47*, 17392–17400; g) M. Strianese, D. Guarnieri, M. Lamberti, A. Landi, A. Peluso, C. Pellecchia, *Inorg. Chem.* **2020**, *59*, 15977–15986.
[8] a) W. P. Lustig, S. Mukherjee, N. D. Rudd, A. V. Desai, J. Li, S. K. Ghosh, *Chem. Soc. Rev.* **2017**, *46*, 3242–3285; b) K. Vikrant, V. Kumar, Y. S. Ok, K.-H. Kim, A. Deep, *TrAC Trends Anal. Chem.* **2018**, *105*, 263–281; c) H.-Y. Li, S.-N. Zhao, S.-Q. Zang, J. Li, *Chem. Soc. Rev.* **2020**, *49*, 6364–6401; d) T. Islamoglu, Z. Chen, M. C. Wasson, C. T. Buru, K. O. Kirlikovali, U. Afrin, M. R. Mian, O. K. Farha, *Chem. Rev.* **2020**, *120*, 8130–8160.
[9] a) S. S. Nagarkar, A. V. Desai, S. K. Ghosh, *Chem. Eur. J.* **2015**, *21*, 9994–9997; b) Z. Zhu, X. He, W.-N. Wang, *CrystEngComm* **2020**, *22*, 195–204; c) X. Han, C. Gu, Y. Ding, J. Yu, K. Li, D. Zhao, B. Chen, *ACS Appl. Mater. Interfaces* **2021**, *13*, 20371–20379; d) Y. Li, X. Zhang, L. Zhang, K. Jiang, Y. Cui, Y. Yang, G. Qian, *J. Solid State Chem.* **2017**, *255*, 97–101.
[10] R. K. Sharma, M. Agarwal, *J. Environ. Biol.* **2005**, *26*, 301–313.
[11] a) R. Moi, K. Nath, K. Biradha, *Chem. Asian J.* **2019**, *14*, 3742–3747; b) S. K. Konavarapu, A. Goswami, A. G. Kumar, S. Banerjee, K. Biradha, *Inorg. Chem. Front.* **2019**, *6*, 184–191; c) K. Nath, K. Maity, K. Biradha, *Cryst. Growth Des.* **2017**, *17*, 4437–4444.
[12] a) X.-L. Wang, Y. Xiong, X.-T. Sha, G.-C. Liu, H.-Y. Lin, *Cryst. Growth Des.* **2017**, *17*, 483–496; b) X.-L. Wang, Y. Xiong, G.-C. Liu, H.-Y. Lin, X. Wang, *Dalton Trans.* **2018**, *47*, 9903–9911; c) Y. Xiong, G.-C. Liu, X.-L. Wang, J. Zhang, H.-Y. Lin, X.-T. Sha, *CrystEngComm* **2017**, *19*, 4561–4570.
[13] a) S. S. Nagarkar, T. Saha, A. V. Desai, P. Talukdar, S. K. Ghosh, *Sci. Rep.* **2014**, *4*, 7053–7058; b) S. Nandi, H. Reinsch, S. Banesh, N. Stock, V.

Trivedi, S. Biswas, *Dalton Trans.* **2017**, *46*, 12856–12864; c) A. Legrand, A. Pastushenko, V. Lysenko, A. Geloen, E. A. Quadrelli, J. Canivet, D. Farrusseng, *ChemNanoMat* **2016**, *2*, 866–872; d) C. Yang, K. Chen, M. Chen, X. Hu, S.-Y. Huan, L. Chen, G. Song, X.-B. Zhang, *Anal. Chem.* **2019**, *91*, 2727–2733.

[14] a) X. Xin, J. Wang, C. Gong, H. Xu, R. Wang, S. Ji, H. Dong, Q. Meng, L. Zhang, F. Dai, D. Sun, *Sci. Rep.* **2016**, *6*, 21951–21959; b) X.-F. Wang, H.-B. Zhu, M. Liu, *Inorg. Chim. Acta* **2017**, *466*, 410–416.

[15] a) H. Li, X. Feng, Y. Guo, D. Chen, R. Li, X. Ren, X. Jiang, Y. Dong, B. Wang, *Sci. Rep.* **2014**, *4*, 4366–4370; b) X. Zhang, J. Zhang, Q. Hu, Y. Cui, Y. Yang, G. Qian, *Appl. Surf. Sci.* **2015**, *355*, 814–819; c) Y.-Y. Cao, X.-F. Guo, H. Wang, *Sens. Actuators B* **2017**, *243*, 8–13; d) X. Zhao, L. Zhang, J. Bai, P. Wu, Y. Li, L. Liang, L. Xie, J. Wang, *Spectrochim. Acta Part A* **2020**, *243*, 118794–118799.

Manuscript received: October 24, 2021
Accepted manuscript online: December 22, 2021
Version of record online: January 19, 2022